A Compact Dual-Band Pattern Diversity Antenna by Dual-Band Reconfigurable Frequency-Selective Reflectors With a Minimum Number of Switches

— **Source link** ↗

Chih-Hsiang Ko, I-Young Tarn, Shyh-Jong Chung

Institutions: National Chiao Tung University, National Space Organization

Topics: Reconfigurable antenna, Reflector (antenna), Corner reflector antenna, Antenna measurement and Antenna (radio)

Related papers:

- A Novel Pattern Diversity Reflector Antenna Using Reconfigurable Frequency Selective Reflectors

- A Novel Pattern-Reconfigurable Antenna Using Switched Printed Elements

- A novel compact wideband reflector antenna with reconfigurable radiation patterns

- Frequency and Pattern Reconfigurable Slot Antenna

- A novel reconfigurable antenna based on active band reflective frequency selective surface

Share this paper: ❋ 🐦 in ✉

A Compact Dual-Band Pattern Diversity Antenna by Dual-Band Reconfigurable Frequency-Selective Reflectors With a Minimum Number of Switches

Chih-Hsiang Ko, I.-Young Tarn, and Shyh-Jong Chung, *Senior Member, IEEE*

Abstract—A novel compact dual-band pattern diversity antenna is proposed. Dual-band reconfigurable frequency-selective reflectors are designed and applied to form a right-angle corner reflector antenna with reconfigurable patterns. With only one switch, the reconfigurable frequency-selective reflector can be controlled to be transmissive or reflective to vertically polarized waves at 2.45 and 5.25 GHz. By changing the combinations of the switch states, multiple patterns can be obtained. A dual-band feeding antenna designed via using the coupling effects is made to achieve well-matching conditions in all circumstances corresponding to various switch states at both frequencies. The measured results show good agreement with the calculated ones and demonstrate good pattern diversity virtues.

Index Terms—Corner reflector antenna, dual band, pattern diversity, reconfigurable frequency-selective reflector.

I. INTRODUCTION

THE OPERATION frequencies for the IEEE 802.11 a/b/g/n are one of the most crowded bands in wireless communications since they are unlicensed by any international agreement or government authority. Therefore, efficiently utilizing the limited spectrum in such bands is very crucial and indispensable. Many solutions in relative fields have been proposed or under development. The pattern diversity antenna is a good candidate to solve the problem and mitigate the multipath effects [1], [2]. Its radiation pattern can be shaped to concentrate the energy to the directions of targets and minimize the gain in unwanted directions. Generally, an omnidirectional pattern is also provided to communicate in all directions. The most suitable pattern can be configured on demand with the pattern-reconfigurable antenna.

Numerous pattern-reconfigurable antennas stemmed from the variations of the Yagi-Uda antenna [4]–[8]. When the length of the parasitic element is shorter than that of the active element, a pulling pattern is obtained. On the other hand, if the length of the parasitic one is longer than that of the active element, a pushing pattern is formed. Therefore, different arrangements of

parasitic elements with different lengths around the active element yield different radiation patterns. This offers a simple and flexible method for beamforming. However, in order to have pattern reconfiguration, their designs need to place switches on the reflectors or directors, and they may severely affect the radiation patterns when real switches are implemented.

Another way to construct pattern-reconfigurable antennas is using the switched arrays [9]–[12]. A phase array can change the main beam direction by appropriately adjusting the feeding phases of the active elements. In [11], adequate phases to the antennas are accomplished by shifting the feeding point of the power divider. The main beam direction varies with frequencies because the phase differences between paths change with frequencies, whereas in [12], the distribution of phase angles at each port of the feeding network can be altered by moving the metal-coated slab. Other than these two types of reconfigurable antennas, a radiation pattern diversity antenna, which combines the concept of the reconfigurable frequency-selective reflector (RFSR) and the right-angle corner reflector antenna [13], was devised by the authors recently.

The aforementioned pattern-reconfigurable antennas are available only in single band, and the sizes are comparatively large. In this paper, a compact dual-band pattern-reconfigurable antenna is introduced. A novel dual-band RFSR is created to develop a dual-band pattern-reconfigurable corner reflector antenna. The dimensions of the proposed antenna are very small. The size in each dimension is less than $\lambda/2$ of the lower frequency. The transmission and reflection characteristics of the RFSR at 2.45 GHz and 5.25 GHz are designed to be controlled by only one switch. That is, four switches are enough to configure the reflection states of the side walls of the antenna, in order to adaptively form the radiation patterns. The switching circuits and the impedance-matching networks can be hidden beneath the ground plane to prevent the unwanted influences on electromagnetic waves. Moreover, this antenna features beam tilting property inherently, which is suitable for up-to-down communication. For example, this antenna can be mounted on ceilings in a room to transmit and receive signals from users in the same room. By virtue of its compact size, dual-band operation, and simple control scheme, the proposed antenna is particularly suitable for base-station antenna applications in modern wireless communication systems.

II. DESIGN

The proposed dual-band pattern-reconfigurable antenna by the RFSRs is shown in Fig. 1. It consists of a dual-band feeding
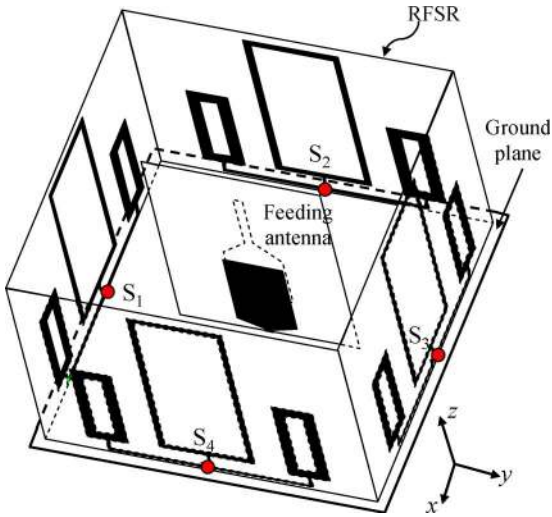
Fig. 1. Configuration of the proposed dual-band pattern diversity antenna by single-layer RFSRs.

antenna in the center, four dual-band RFSRs on the side walls, and a finite-square ground plate on which the feeding antenna and RFSRs are perpendicularly mounted. Each dual-band RFSR has two groups of rectangular loops. The transmission and reflection properties of the RFSRs are controlled by four switches $S_1 \sim S_4$. In one switch state, both groups of rectangular loops are at resonance when excited by vertically polarized incident waves at the two resonant frequencies and, thus, the waves will be reflected. In the other switch state, those rectangular loops are out of resonance, so they are transparent to waves. Only one switch is needed for each dual-band reflector. Multiple radiation patterns can be achieved according to the combinations of the switch states.

The ground plane is on the top surface of an FR4 laminate. The dual-band feeding antenna is located at the center of the ground plate and designed for operating at 2.45 and 5.25 GHz. The matching circuit for the feeding antenna can be printed on the bottom side of the ground substrate if necessary. In our work, a feeding antenna, which has relatively broad bandwidths around both frequencies, was used. Hence, no additional impedance-matching network is required, which greatly simplifies the antenna design.

Moreover, the associate circuits for the switches can also be fabricated underneath the ground plane. This advantage makes the design much easier since it can avoid the undesired electromagnetic interactions between the antenna and the circuits.

A. Antenna Size

To design the proposed antenna, the spacing between the feeding antenna and the reflecting wall of a corner reflector antenna should be first determined. Then, the widths of the reflectors and the dimensions of the ground can be determined accordingly. Fig. 2(a) shows the structure model used to determine the spacing. Two metal plates with a height of 40 mm are vertically mounted on the ground. The distance between the wall and the feeding antenna is denoted as d. The width of these metal walls is equal to twice the amount of spacing $2d$. The
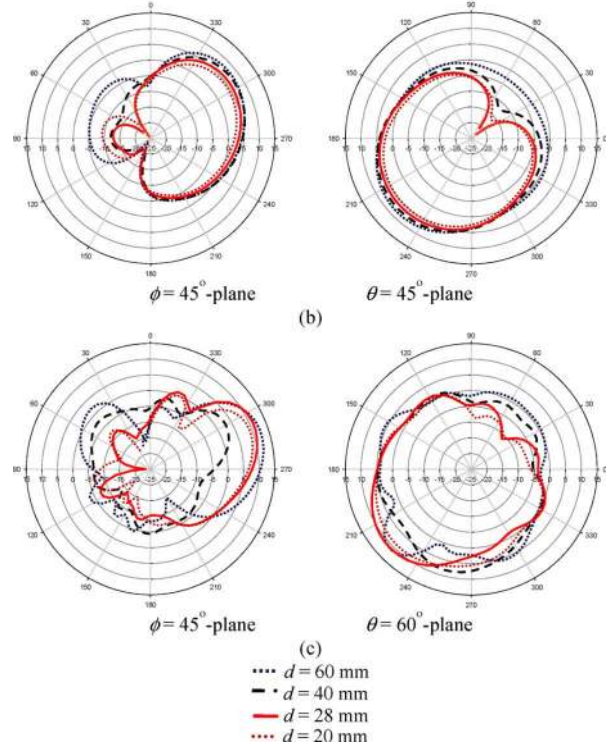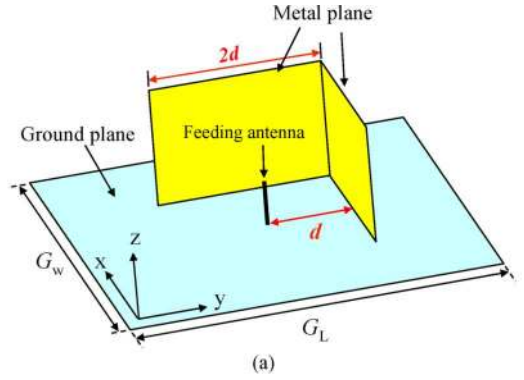

Fig. 2. (a) The structure model used to determine the spacing d between the active element and the reflecting wall, and the simulated radiation patterns at (b) 2.45 GHz and (c) 5.25 GHz.

dimensions of the ground plate (G_W, G_L) are fixed to be (140 mm, 140 mm) in this phase. The simulated radiation patterns for different spacings are shown in Fig. 2(b) and (c) for 2.45 GHz and 5.25 GHz, respectively. It is found that the maximum gain and the shapes of the patterns at 5.25 GHz vary much with d, whereas the patterns at 2.45 GHz are almost independent of d. It is better to make the antenna as small as possible. In addition, the sidelobe and backlobe levels are an important issue in a directional antenna. The patterns for $d = 40$ mm and $d = 60$ mm have inferior performances in terms of the front-to-back ratio, and the case with $d = 20$ mm has slightly lower directivity. Hence, by considering the aforemtioned factors, the spacing d of 28 mm is chosen.

B. Dual-Band Reconfigurable Frequency-Selective Reflector

The geometry of the dual-band RFSR is shown in Fig. 3, which contains a center large rectangular loop for 2.45 GHz and
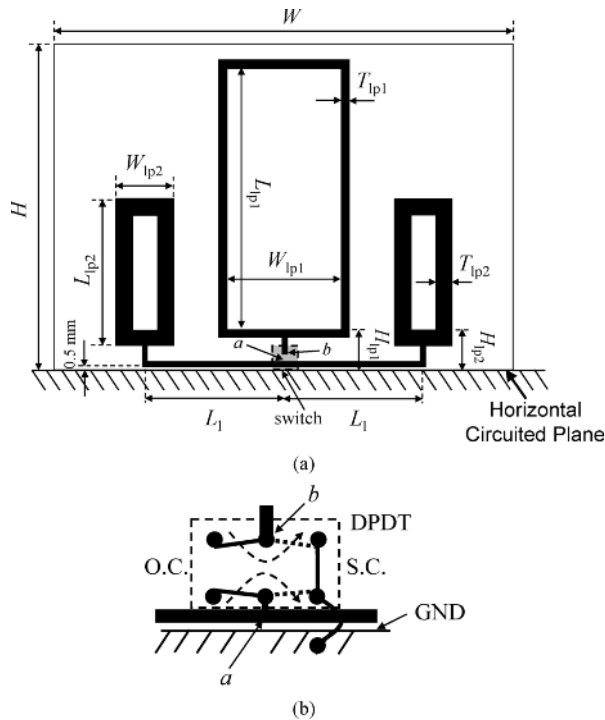
Fig. 3. (a) Geometry of the proposed dual-band RFSR. (b) Geometry of the DPDT switch.
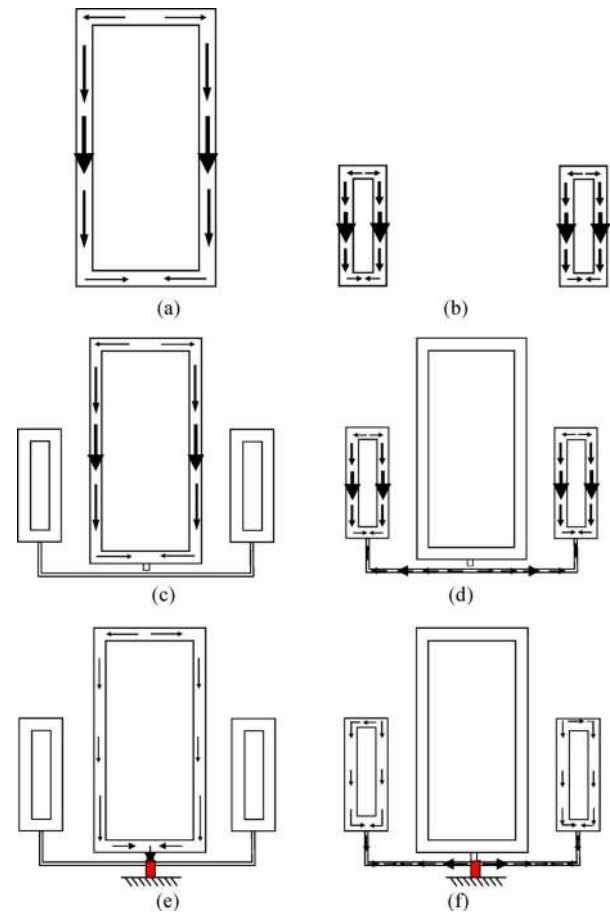

Fig. 4. Induced currents (a) on the center large loop at 2.45 GHz, (b) on one of the side small loop at 5.25 GHz, (c) on the dual-band RFSR in the offstate at 2.45 GHz, (d) on the dual-band RFSR in the offstate at 5.25 GHz, (e) on the dual-band RFSR in the onstate at 2.45 GHz, and (f) on the dual-band RFSR in the onstate at 5.25 GHz.

two side small loops for 5.25 GHz. The two small loops are connected by two side short vertical lines and a horizontal line of length $2L_1$. Notice that the horizontal line is close to the ground plane, with a spacing of only 0.5 mm. Therefore, together with the ground plane, it forms a transmission line. For the central large loop, there is one central short line connected to the lower midpoint of the large loop. A double-pole-double-throw switch (DPDT) [14] is mounted on the backside of the RFSR to connect the center point a of the horizontal line, the end point b of the short vertical line, and the ground, where the point a and the point b are connected to the upper and lower input of the DPDT. When the control signal is "on," both points a and b are switched to the right, which is short-circuited to the ground. On the other hand, when the control signal is "off," both points are switched to the left, which are open-circuited. Through different states at the two points, the transmissive and reflective states can be controlled. According to the design in the previous subsection, the width W and the height H of the RFSR are set as 56 and 40 mm, respectively. In principle, the perimeter of a loop-type resonator should be about 1 λ of the operating frequency [16], [17]. In this paper, the wave component excited by the feeding antenna is mainly vertically polarized. Thus, the lengths of the rectangular loops (L_{lp1}, L_{lp2}) must be longer than the widths (W_{lp1}, W_{lp2}). The length and width of the center large loop (L_{lp1}, W_{lp1}) are (36 mm, 18 mm), respectively, while those of the side small loops (L_{lp2}, W_{lp2}) are (18 mm, 7 mm). The perimeter of the center large loop is 108 mm, and that of the side small loops is 50 mm. They are about 1 λ of 2.45 GHz and 5.25 GHz, respectively.

The current distributions on these loops change significantly with the switch states, so their frequency responses are quite different in different switch states. Initially, consider only the center large loop and the side loop, but without the short vertical lines and the horizontal transmission line, as shown in Fig. 4(a) and (b). Because of the symmetry in geometry and the 1λ perimeter, when vertically polarized plane waves at resonant frequencies impinge on the loops, current nulls appear at the midpoints of the top and bottom horizontal segments of the loops, and strong in-phase currents occur at the midpoints of the vertical segments. Then, the re-radiated fields excited from the induced currents would cancel the incoming waves at the backside of the reflector while generating a wave propagating toward the opposite direction. Hence, the RFSR structures reflect the incident waves back.

Next, consider the existence of the transmission line and the vertical short lines. In Fig. 4(c), the end point b of the central short line connecting the bottom middle point of the center large loop is open-circuited if the switch is off. When a vertically polarized plane wave at 2.45 GHz is incident on the center large loop, the open-circuit condition extends to the bottom middle point of the center loop because the length of the vertical line is relatively short compared with the wavelength of 2.45 GHz. As a result, the resonant current distribution excited by the incident wave remains as the one without the transmission line, and
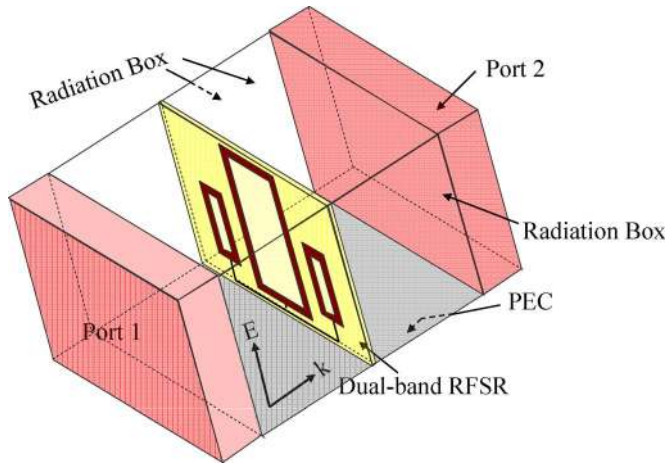
Fig. 5. Simulation model for designing the dual-band RFSR.

Fig. 6. Simulated OFF-state transmission coefficients for various heights of (a) the center loop and (b) the two side loops.

the incident waves will be reflected. In order to minimize the number of switches, we built a mechanism to configure the two groups of rectangular loops in the same state with one switch. When a vertically polarized wave at 5.25 GHz is incident, due to the geometrical symmetry of the horizontal transmission line, an open circuit appears at the midpoint of this line when the switch is off. On the purpose of generating open circuits at both ends of the horizontal line, a 1λ-long transmission line at 5.25 GHz is required. According to the transmission-line theory, the open-circuit condition will show at the two ends of the line through the half-wavelength transformation at each side. As a result, the resonant current distribution excited by 5.25-GHz vertically polarized incident waves remains the same as the one without the transmission line, and incident waves will be reflected. The induced currents on the side small loops remain resonant, as shown in Fig. 4(d). Consequently, the RFSR is reflective at 2.45 GHz and 5.25 GHz when the switch is OFF.

On the other hand, when the switch is on, the end of the central short line and the midpoint of the horizontal transmission line is short-circuited to ground. Nearly short-circuit conditions show at the bottom middle point of the center loop and at both ends of the horizontal line, which thus destroy the resonance requirement for both two types of loops. As shown in Fig. 4(e) and (f), the induced currents will become weak and out of resonance, so that the re-radiated fields can be ignored. Consequently, the incoming waves will pass through the RFSR.

In brief, in the "OFF-state" of the switch, a vertically polarized incident wave will be reflected by the RFSR, and in the "ON-state," the wave will pass through the RFSR.

The full-wave electromagnetic software Ansoft HFSS [18] was employed to analyze this dual-band RFSR. The simulation model is shown in Fig. 5. A perfectly conducting condition is applied on the ground plane, and the other three surfaces are assigned to be radiation boundaries to emulate open-region radiation. The vertically polarized plane wave was excited from one of the two ports and incident upon the RFSR at the center of the model. The transmission coefficients (S_{21}) in the situation without RFSR at the center were taken as the reference. Then, S_{21} with the RFSR structure inserted were simulated and compared to the reference to obtain the transmission coefficients of the RFSR.
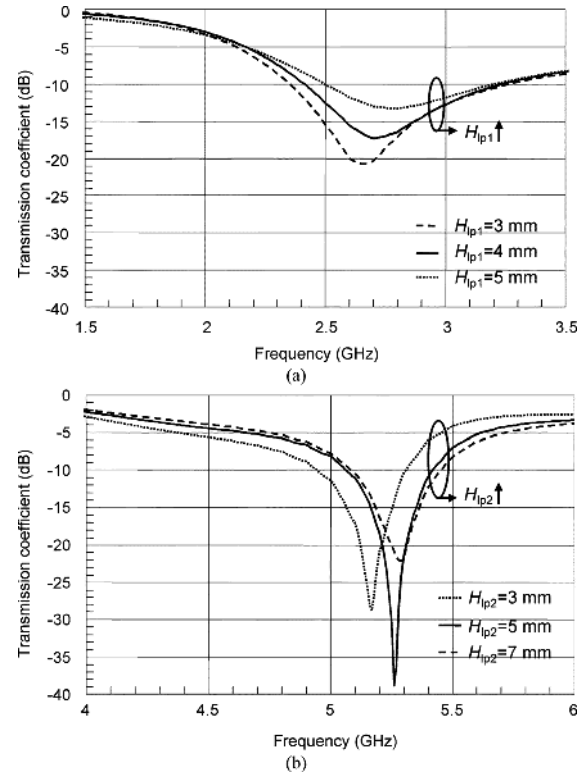
There are some parameters other than the dimensions of the loops affecting the operating frequencies and the bandwidths of the RFSR. It can be seen in Fig. 6 that the transmission coefficients vary with the height (H_{lp1}, see Fig. 3) of the center large loop and that (H_{lp2}) of the two side small loops. The effect of the thicknesses ($T_{\text{lp1}}, T_{\text{lp2}}$) of the loops is shown in Fig. 7. For 2.45 GHz, in Fig. 7(a), T_{lp1} does not affect the resonant frequency but the bandwidth. However, the influence of T_{lp2} for 5.25 GHz is severe. When T_{lp2} increases, the resonant frequency goes lower while the bandwidth increases, as shown in Fig. 7(b). The difference of the effects is because the variations of the thickness of the loops are comparatively large to higher resonant frequency. In addition, the transmission coefficients for various L_l (half length of the horizontal transmission line) are displayed in Fig. 8. The resonant frequency decreases with increasing L_l.

With the aforementioned observations and the consideration of the $\lambda/2$ transmission line for 5.25 GHz, ($H_{\text{lp1}}, T_{\text{lp1}}$) for the center large loop are determined to be (4.5 mm, 2 mm), and ($H_{\text{lp2}}, T_{\text{lp2}}, L_l$) for the side small loop are (6 mm, 2 mm, 17 mm). The simulated transmission coefficients of the finalized RFSR are shown in Fig. 9. The transmission coefficients at both frequencies in the ON-state are higher than -3 dB while those in the OFF-state are lower than -10 dB. Note that "ON-state" means that the switch is on while the "OFF-state" indicates that the switch is off. Good transmission in the ON-state and good reflection in the OFF-state are achieved for both 2.45- and 5.25-GHz frequency bands. It is noticed that due to the leakage of the incident wave at the radiation boundaries, the transmission coefficients in the ON-state would not reach 0 dB. The maximum
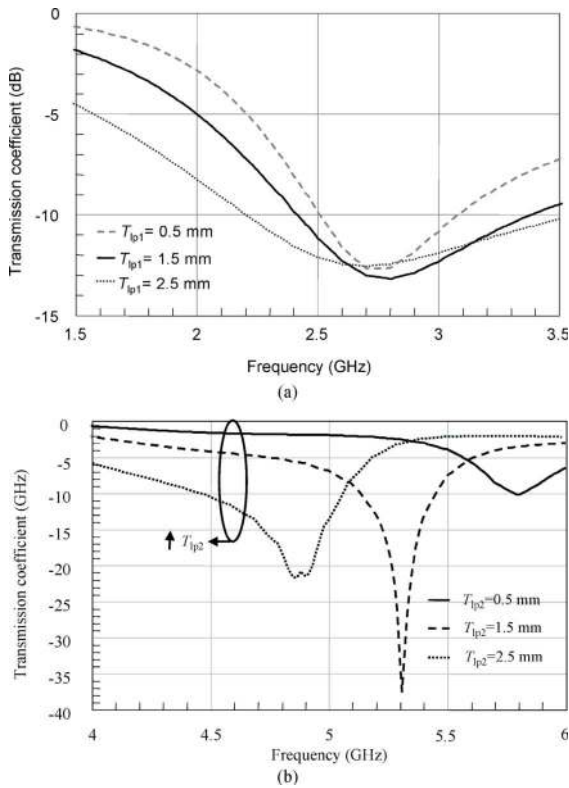
Fig. 7. Simulated OFF-state transmission coefficients for various thicknesses of (a) the center loop and (b) the two side loops.
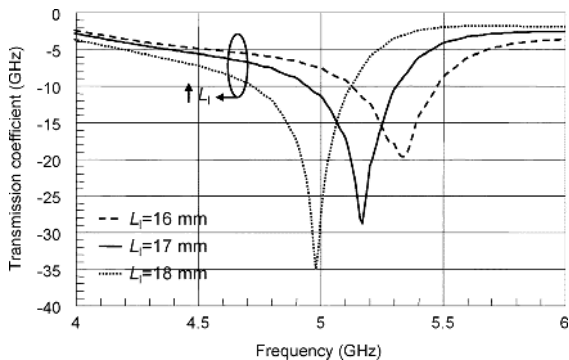

Fig. 8. Simulated OFF-state transmission coefficients for various L_1.

values occur at the two operation bands, which are -2.5 dB and -3 dB for the lower and higher bands, respectively.

The simulated current distributions in the ON- and OFF-state at 2.45 GHz and 5.25 GHz are shown in Fig. 10. The induced currents in the OFF-state are much stronger than in the ON-state, even though the opens do not exactly occur at the connecting points due to the coupling effect [13]. However, the main current distribution remains as the one without the transmission lines and, thus, the reflective effects on a vertically polarized incident wave in the OFF-state still remain.

An important thing is that the large loop should not be directly connected to the horizontal transmission line when the switch is off. Otherwise, the center large loop provides a grounding condition at the midpoint (point a) of the horizontal transmission line because it is comparatively large for a 5.25-GHz incident wave. This grounding condition will, in turn, appear at the two
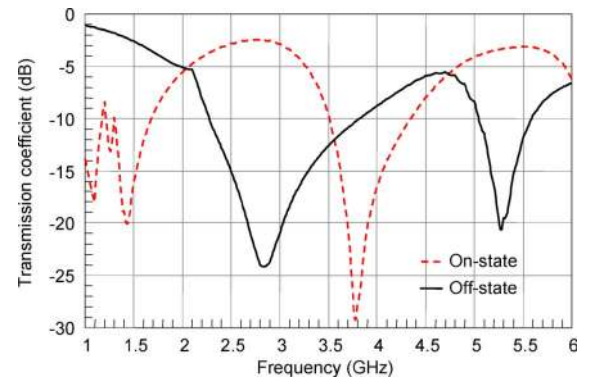

Fig. 9. Simulated transmission coefficients of the proposed dual-band RFSR in the ON-state and OFF-state.
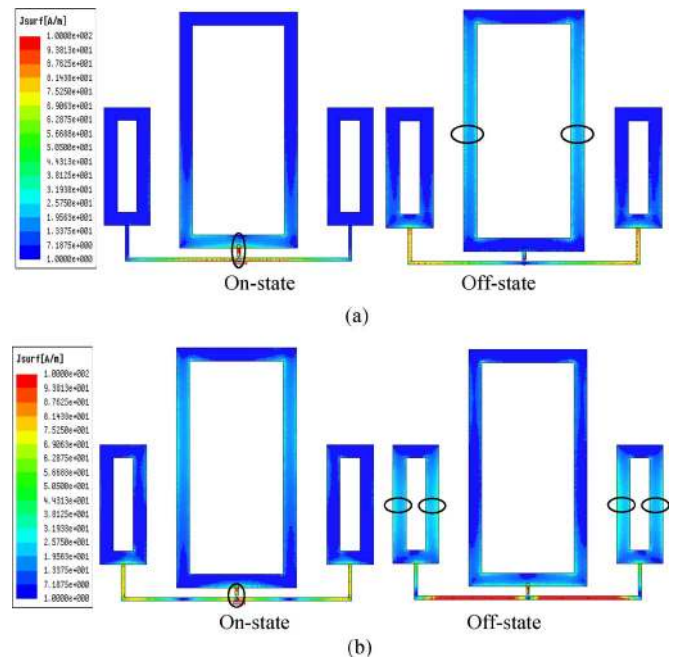

Fig. 10. Simulated current distributions on the RFSR in the ON- and OFF-state at (a) 2.45 GHz and (b) 5.25 GHz.

ends of the transmission line and, thus, destroys the resonance requirement for the small loops at 5.25 GHz. Fig. 11 shows the current distribution and the transmission coefficient of the RFSR when the large loop is directly connected to the midpoint of the horizontal transmission line. It is observed that the currents are mainly distributed along the transmission line. Only negligible currents appear at the loops. It is also found from Fig. 11(b) that under this condition, the RFSR no longer reflects the 5.25-GHz incident wave. Thus, a DPDT switch is applied to accommodate the necessary current separation between the two transmission lines when in the OFF-state.

C. Dual-Band Feeding Antenna

A dual-band feeding antenna that is less sensitive to the environment is required to maintain good impedance matching in different surrounding conditions caused by the combinations of the reflection states of the sidewalls. It is hard to use an impedance-matching network to satisfy the various radiating conditions at two frequencies. In this paper, the lower resonant
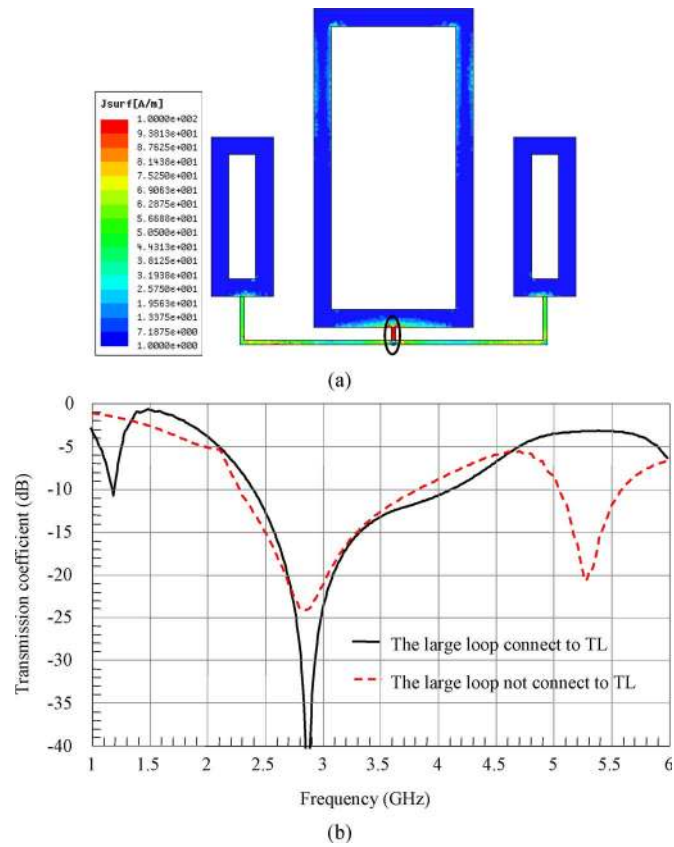
(a)

(b)

Fig. 11. (a) Simulated current distribution on the RFSR at 5.25 GHz when the two transmission lines are connected. (b) The transmission coefficients with the central short and horizontal lines connected and disconnected.
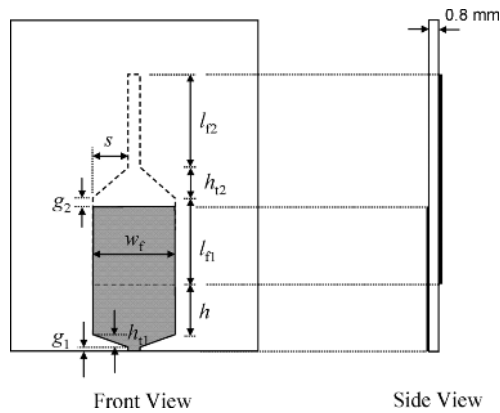

Fig. 12. Geometry of the dual-band feeding antenna.

frequency of the dual-band feeding antenna is designed to be excited by couplings, which have relatively broad bandwidths at dual bands than by the conventional direct feeding method [15]. Thus, acceptable return losses at the desired frequencies can be achieved for various switch states.

The proposed dual-band feeding antenna is shown in Fig. 12. It has two parts printed on both sides of a 0.8-mm-thick, 30-mm-wide and 40-mm-long FR4 substrate. The front part directly excites the higher frequency radiation while the back part combined with the former by coupling effects resonates at the lower frequency. The suitable amount of coupling can be obtained by
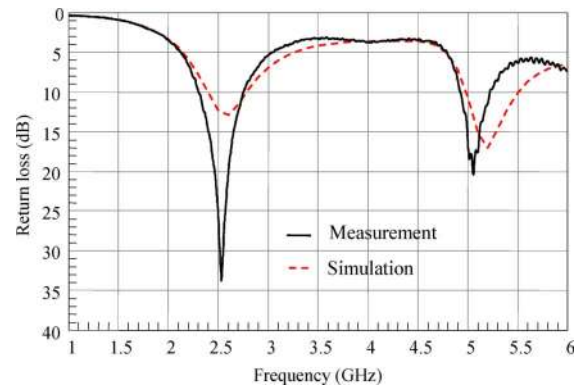

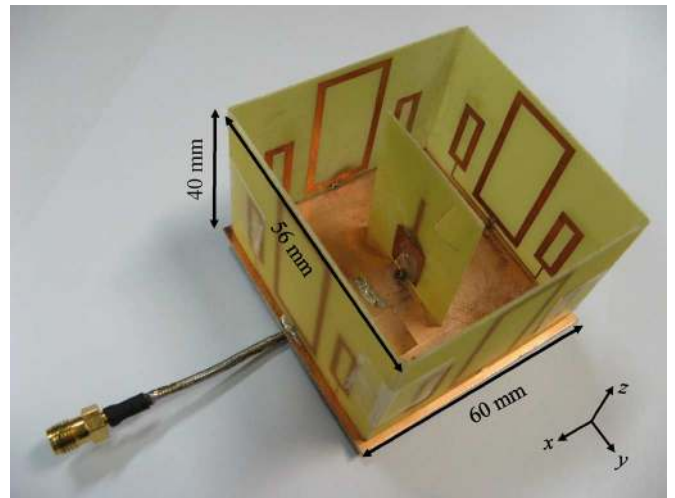Fig. 13. Measured and simulated return loss of the dual-band feeding antenna.

Fig. 14. Picture of the realized dual-band pattern-reconfigurable antenna.

adjusting w_f, h and g_2. The optimized geometry parameters are as follows: $h = 2$ mm, $h_{t1} = 1.5$ mm, $h_{t2} = 3.75$ mm, $l_{f1} = 10.5$ mm, $l_{f2} = 11.25$ mm, $s = 4.25$ mm, $w_f = 10$ mm, $g_1 = 0.5$ mm, and $g_2 = 0$ mm. The total height of the front part and the back part is 29.5 mm $(g_1 + h_{t1} + h + l_{f1} + h_{t2} + L_{f2})$, and the height of the front part is 14.5 mm $(g_1 + h_{t1} + L_{f1})$, which are about $\lambda/4$ of the two operating frequencies, respectively. The measured and simulated return losses are shown in Fig. 13. In the lower frequency band, the measured 10-dB bandwidth is from 2.31 to 2.76 GHz, and the best return loss occurs at 2.55 GHz. In the higher band, the measured bandwidth is between 4.92 and 5.22 GHz while the simulated one is between 4.98 and 5.50 GHz. A slight frequency shift occurs in the higher frequency region, which might be caused by fabrication.

III. MEASUREMENT RESULTS

The realized dual-band pattern-reconfigurable antenna is shown in Fig. 14. The entire antenna structure occupies a volume of $60 \times 60 \times 40.8$ mm ^{3}. First, the ideal short and open circuit were implemented to represent the ON- and OFF-state of the DPDT switch. Two of the operating modes of the antenna are noteworthy: "Case 1" has a directional pattern, and "Case 2" is the one with an omnidirectional pattern.

TABLE I
DEFINITIONS OF CASE 1 AND CASE 2 AND THE SIMULATED AND MEASURED
RESULTS OF THE DUAL-BAND PATTERN DIVERSITY ANTENNA

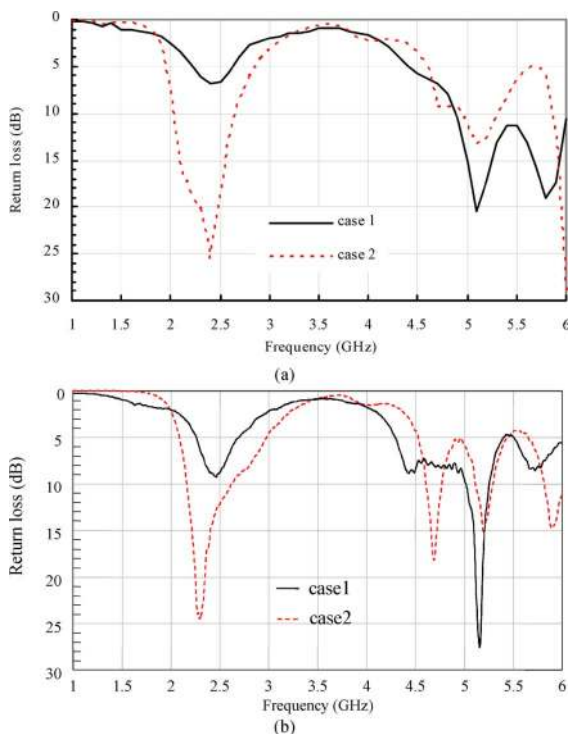|	Switch	Case1	Case2
	S_1	Off	On
	S_2	Off	On
	S_3	On	On
	S_4	On	On
Simulated peak gain direction	2.55GHz	$\theta = 65^\circ$ $\phi = 45^\circ$	Omni
	5.25GHz	$\theta = 40^\circ$ $\phi = 45^\circ$	Omni-like
Simulated peak gain(dBi)	2.55GHz	4.27	2.01
	5.25GHz	7.81	4.3
Measured peak gain direction	2.55GHz	$\theta = 45^\circ$ $\phi = 45^\circ$	Omni
	5.25GHz	$\theta = 30^\circ$ $\phi = 45^\circ$	Omni-like
Measured peak gain(dBi)	2.55GHz	3.54	2.08
	5.25GHz	7.77	4.67

Fig. 15. (a) Simulated return loss of the proposed antenna. (b) Measured return loss of the proposed antenna.

Fig. 16. Measured and simulated radiation patterns in the $\phi = 45^\circ$-plane of Case 1 at (a) 2.55 GHz. and (b) 5.25 GHz.

In practical applications, Cases 1 and 2 are the most important ones. The directional pattern can be used to detect the signals, and focus the beam on the desired direction to increase the power and reduce the multipath effects. On the other hand, the omnidirectional pattern can be used to broadcast and receive the signals from almost all directions. The definition of each case and the simulated and measured results are summarized in Table I.
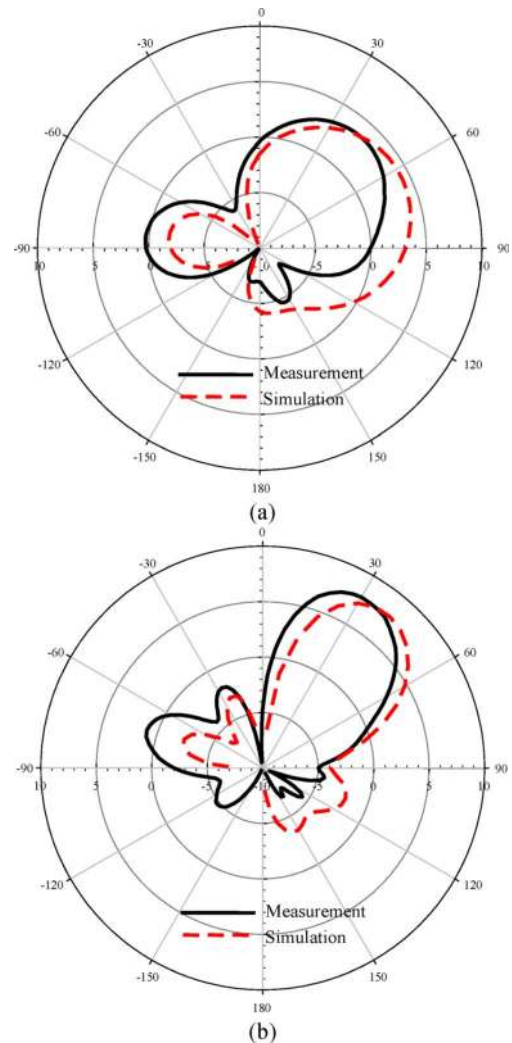
Fig. 15 shows the measured and simulated return losses of Case 1 and Case 2. In both cases, the inband return losses are better than 10 dB, except for the lower band in Case 1 which is still better than 8 dB, which may be tolerable for wireless communications. The measured results show that the coupling feeding structure can alleviate the degradation of matching conditions when the switch changes and retains appropriate radiating power.

The measured radiation patterns of Cases 1 and 2 at 2.55 GHz and 5.25 GHz are shown in Figs. 16 and 17, respectively. In Case 1 (Fig. 16), the maximum gain at 2.55 GHz of 3.54 dBi was measured at $\phi = 45^\circ$ and $\theta = 65^\circ$, and that at 5.25 GHz, it is 7.77 dBi at $\phi = 45^\circ$ and $\theta = 30^\circ$. The front-to-back ratio at 2.5 GHz is 8.31 dBi, and is 9.74 at 5.25 GHz. Therefore, good directivity can be achieved in Case 1, whereas for Case 2, good omnidirectional patterns are observed within $0^\circ < \theta < 60^\circ$. The shape of the omnidirectional pattern is conical above the ground plane in 3-D space. Fig. 17 shows the radiation patterns at the xz- and yz- cuts. In the xz- and yz-plane at 2.55 GHz, the maximum measured gains are $\theta = 60^\circ$ with around 2 dBi and with the 1-dB pattern variations from $\theta = 40^\circ$ to $\theta = 85^\circ$, and at 5.25 GHz, the maximum gains are measured at $\theta = 45^\circ$
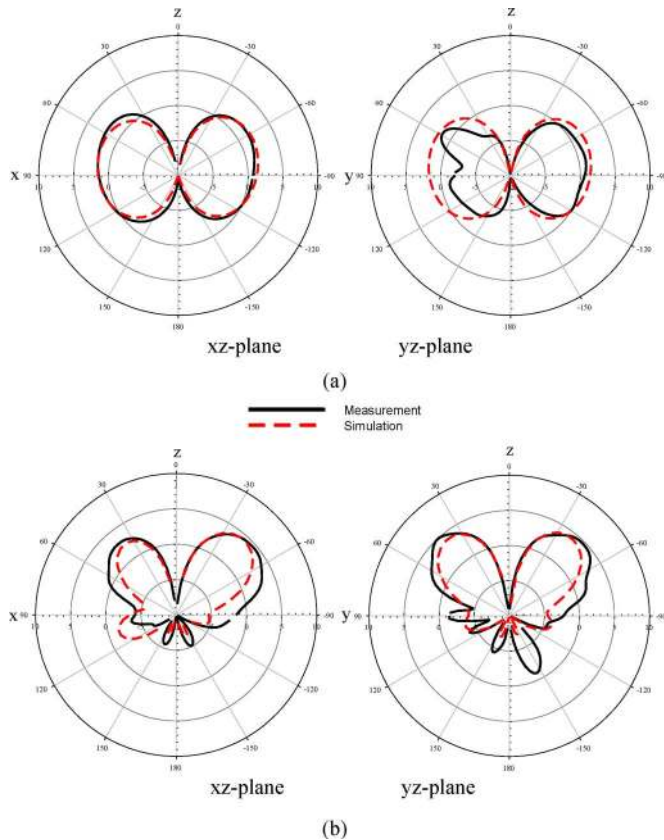
Fig. 17. Measured and simulated radiation patterns in the xz- and yz-plane of Case 2 at (a) 2.55 GHz and (b) 5.25 GHz.

with the values at about 4.5 dBi and with the 1-dB pattern variations from $\theta = 40°$ to $\theta = 50°$. At the $\theta = 60°$ and $\theta = 45°$ plane for 2.55 GHz and 5.25 GHz respectively, the pattern variations of both operating bands are small and, thus, omnidirectional patterns at both bands can be achieved in Case 2. The measured patterns for both cases at both frequency bands agree with the simulated ones in the main beam region, but with dissimilar side-lobes because of the error occurring at manual fabrication. For instance, the gap between the horizontal line and the ground plane is only 0.5 mm, which is hard to accurately achieve in the laboratory. The variation of the gap changes the electromagnetic properties of the transmission line, so that the reflection/transmission performance of the RFSR is also affected. Besides, since the proposed antenna is very compact, perfectly mounting the sidewalls and the feeding antenna is very important. The offsets resulting from the fabrication in the laboratory cause the phase errors of the reflecting waves. Therefore, the gain and the main beam direction are deviated from the simulated results. Nevertheless, the proposed antenna still shows good dual-band pattern-reconfiguration properties.

Finally, actual switches were implemented. Every DPDT switch described in Section II-B was realized by two AS225-313 single-pole-double-throw (SPDT) switches [19], as shown in Fig. 18. The switches, together with the associated biasing network and batteries, are installed inside a paper box below the proposed antenna. Fig. 19 shows the measured patterns of Case 1. Compared to Fig. 16, the peak gains of about 3.22 dBi at 2.45 GHz and 7.53 dBi at 5.25 GHz are
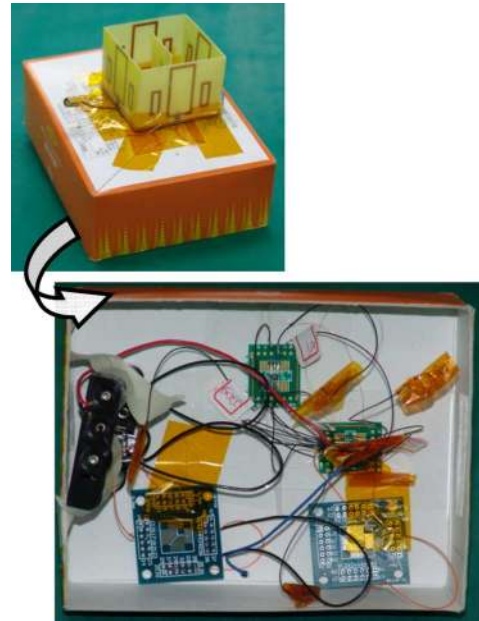

Fig. 18. Picture of the dual-band pattern-reconfigurable antenna with the switch circuits implemented.
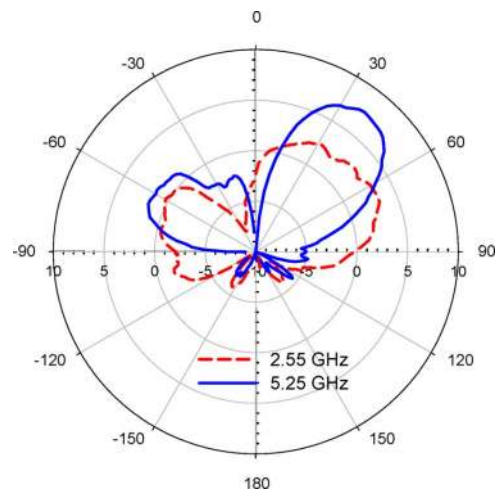

Fig. 19. Measured radiation patterns in the $\phi = 45°$-plane of Case 1 of the proposed antenna with the switch circuits implemented.

slightly reduced. However, the main beams are distorted and the backlobes grow up because the rectangular loops on the RFSR in the ON-state are more poorly shorted to the ground through the switches. Also, the existence of the biasing circuits deteriorates the radiation patterns.

IV. CONCLUSION

In this paper, a novel compact dual-band pattern diversity antenna has been presented. This antenna combines the corner reflector antenna and dual-band RFSRs. Each dual-band RFSR can be controlled to be transmissive or reflective to waves at a designated frequency with only one switch. The RFSRs are applied on the sidewalls of the corner reflector antenna. The DPDT switch should be used to prevent the unwanted interaction between the center large loop and the small side loops.

With the findings in this paper, it is obvious that the proposed antenna provides diverse patterns in dual frequency bands around 2.55 GHz and 5.25 GHz by configuring the combination of the switch states. The patterns can also be steered to rotate in the azimuth plane. In the directional case (i.e., Case 1), the main lobes pointed toward the direction where the switch states are OFF at both frequencies. They are good enough to enhance the desired signals and minimize the unwanted ones, whereas in Case 2, the omnidirectional case, the proposed antenna has small pattern variations which are good for broadcasting communication.

The work presented in this paper successfully demonstrates the feasibility and performances of the dual-band pattern-reconfigurable antenna with dual-band RFSRs, with the compact size of $60 \times 60 \times 40.8$ mm (smaller than $\lambda/2$ of a lower frequency), which is easy to integrate into many wireless communication systems.

REFERENCES

[1] F. Thudor and A. Louzir, "An extremely compact pattern diversity antenna for WLAN," in *Proc. IEEE AP-S Int. Symp.*, Jul. 2005, pp. 589–592.

[2] M. G. Douglas and R. H. Johnston, "A compact two way diversity microstrip upatch antenna," in *Proc. IEEE AP-S Int. Symp. Dig.*, Jun. 1995, vol. 2, pp. 978–981.

[3] A. Mehta and D. Mirshekar-Syahkal, "Spiral antenna with adaptive radiation pattern under electronic control," in *Proc. IEEE AP-S Int. Symp.*, Jun. 2004, vol. 1, pp. 843–846.

[4] S. Zhang, G. H. Huff, J. Feng, and J. T. Bernhard, "A pattern reconfigurable microstrip parasitic array," *IEEE Trans. Antennas Propag.*, vol. 52, no. 10, pp. 2773–2776, Oct. 2004.

[5] R. Schlub and D. V. Thiel, "Switched parasitic antenna on a finite ground plane with conductive sleeve," *IEEE Trans. Antennas Propag.*, vol. 52, no. 5, pp. 1343–1347, May 2004.

[6] C. Laohapensaeng, C. Free, and K. M. Lum, "Printed strip monopole antenna with the parasitic elements on the circular ground plane," in *Proc. IWAT Int. Workshop*, Mar. 2005, pp. 371–374.

[7] L. Low and R. J. Langley, "Single feed antenna with radiation pattern diversity," *Inst. Elect. Eng. Electron. Lett.*, vol. 40, no. 16, pp. 975–976, Aug. 2004.

[8] Y. Ding, Z. Du, K. Gong, and Z. Feng, "A novel dual-band printed diversity antenna for mobile terminals," *IEEE Trans. Antennas Propag.*, vol. 55, no. 7, pp. 2088–2096, Jul. 2007.

[9] C. A. Reddy, K. V. Janardhanan, K. K. Mukundan, and K. S. V. Shenoy, "Concept of an interlaced phased array for beam switching," *IEEE Trans. Antennas Propag.*, vol. 38, no. 4, pp. 573–575, Apr. 1990.

[10] R. C. Reinhart, S. K. Johnson, R. J. Acosta, and S. Sands, "Phase array antenna-based system degradation at wide scan angles," in *Proc. PAST Int. Symp.*, Oct. 2003, pp. 446–451.

[11] M. Barba, J. E. Page, J. A. Encinar, and J. R. M. Garai, "A switchable multiple beam antenna for GSM-UMTS base stations in planar technology," *IEEE Trans. Antennas Propag.*, vol. 54, no. 11, pp. 3087–3094, Nov. 2006.

[12] R. B. Hwang, Y. J. Chang, and M. I. Lai, "A low-cost electrical beam tilting base station antennas for wireless communication system," *IEEE Trans. Antennas Propag.*, vol. 52, no. 1, pp. 115–121, Jan. 2004.

[13] I. Y. Tarn and S. J. Chung, "A novel pattern diversity reflector antenna using reconfigurable frequency selective surfaces," *IEEE Trans. Antennas Propag.*, vol. 57, no. 10, pt. 2, pp. 3035–3042, Oct. 2009.

[14] MA-COM Technology Solutions, Inc., Lowell, MA, MASW2040 GaAs DPDT Switch. [Online]. Available: http://www.macomtech.com/datasheets/MASW2040.pdf

[15] Y. Y. Wang and S. J. Chung, "A new dual-band antenna for WLAN applications," in *Proc. IEEE AP-S Int. Symp.*, Jun. 20–25, 2004, vol. 3, pp. 2611–2614.

[16] A. Pirhadi, M. Hakkak, F. Keshmiri, and R. K. Baee, "Design of compact dual band high directive electromagnetic bandgap (EBG) resonator antenna using artificial magnetic conductor," *IEEE Trans. Antennas Propag.*, vol. 55, no. 6, pp. 1682–1690, Jun. 2007.

[17] W. L. Stutzman and G. A. Thiele, *Antenna Theory and Design*. New York: Wiley, 1997.

[18] High Frequency Structure Simulator (HFSS). ver. 11.1, Ansoft Corporation, Pittsburgh, PA, Apr. 2008.

[19] Skyworks Solutions, Inc., Woburn, MA, PHEMT GaAs IC 1 W Low Loss 0.1–6 GHz SPDT Switch, Aug. 2006. [Online]. Available: http://www.skyworksinc.com/Uploads/documents/200148C.pdf

Chih-Hsiang Ko was born in Kaohsiung, Taiwan. He received the B.S. and M.S. degrees in communication engineering from National Chiao Tung University, Hsinchu, Taiwan, in 2007 and 2008, respectively.

In 2007, he was an exchange student with the Department of Electrical Engineering, University of Illinois, Urbana-Champaign, IL, USA. He research interests are microwave circuits and antennas.
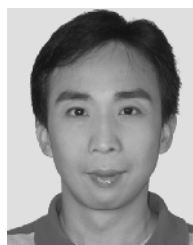
I.-Young Tarn was born in Taipei, Taiwan. He received the B.S. and M.S. degrees in electrical engineering from Yuan-Ze University, Tao-Yuan, Taiwan, in 1993 and 1995, respectively, and is currently pursuing the Ph.D. degree in communication engineering at the National Chiao Tung University, Hsinchu, Taiwan.

From 1995 to 1999, he was an Assistant Researcher in Systems Engineering Project, National Space Program Office, Hsinchu, Taiwan. Since 2000, he has been with the Electrical Engineering Division of the National Space Organization, where he has been involved in satellite communications and antenna design. His research interests include microwave/millimeter-wave planar antennas, reflect array antennas, circular polarization-selective structures, and satellite antenna design and verification.

Shyh-Jong Chung (M'92–SM'06) was born in Taipei, Taiwan. He received the B.S.E.E. and Ph.D. degrees in electrical engineering from National Taiwan University, Taipei, Taiwan, in 1984 and 1988, respectively.

Since 1988, he has been with the Department of Communication Engineering, National Chiao Tung University, Hsinchu, Taiwan, where he is currently a Professor and serves as the Director of the Institute of Communication Engineering. From 1995 to 1996, he was a Visiting Scholar with the Department of Electrical Engineering, Texas, A&M University, College Station. His areas of interest include the design and applications of active and passive planar antennas, LTCC-based RF components and modules, packaging effects of microwave circuits, vehicle-collision warning radars, and communications in intelligent transportation systems (ITSs).

Dr. Chung received the Outstanding Electrical Engineering Professor Award of the Chinese Institute of Electrical Engineering and the Teaching Excellence Awards from National Chiao Tung University both in 2005. He served as the Treasurer of the IEEE Taipei Section from 2001 to 2003 and the Chairman of the IEEE MTT-S Taipei Chapter from 2005 to 2007.